Journal of King Saud University – Science 35 (2023) 102857

HOSTED BY

Contents lists available at ScienceDirect

Journal of King Saud University – Science

journal homepage: www.sciencedirect.com

Original article

Wet chemical synthesis and characterization of $FeVO_4$ nanoparticles for super capacitor as energy storage device

Manal A. Awad [a,*], Awatif A. Hendi [b], Sarala Natarajan [b,c], Khalid M.O. Ortashi [d], Sarah S.A. Alsaif [e], Reema A. Alnamlah [f], Abeer Rasheed [g], Hayat Althobaiti [f]

[a] King Abdullah Institute for Nanotechnology, King Saud University, Riyadh 11451, Saudi Arabia
[b] Department of Physics, College of Science, Princess Nourah bint Abdulrahman University, Riyadh, Saudi Arabia
[c] Department of Physics, Mount Zion College of Engineering & Technology, Pudukkottai, Tamilnadu, India
[d] Department of Chemical Engineering, King Saud University, Saudi Arabia
[e] Department of Botany and Microbiology, King Saud University, Saudi Arabia
[f] Department of Physics and Astronomy, College of Sciences, King Saud University, Saudi Arabia
[g] Department of Chemistry, College of Sciences, King Saud University, Saudi Arabia

ARTICLE INFO

Article history:
Received 3 April 2023
Revised 30 July 2023
Accepted 16 August 2023
Available online 22 August 2023

Keywords:
$FeVO_4$ Nanoparticles
Controlled pH
Specific Capacitance
Paramagnetic Nature

ABSTRACT

Vanadates of transition metal found its potential applications in the fields of lithium ion batteries, gas sensors, photo catalysts, solar cells and so on. Among the metal vanadates, Iron vanadate is vital as an organic pollutant remedying, gas sensor material, and selective catalytic reduction material. This current research focuses on synthesizing iron vanadate nanoparticles by wet chemical synthesis with controlled pH using ammonia solution. The nanostructured $FeVO_4$ particle were characterized structurally with the powder XRD studies. Strong crystal planes were formed at Miller indices (1 1 1), (0–12), and (−2 2 0) which is confirmed from the intensity of the diffraction peaks. FT- IR and micro Raman studies was taken to identify the molecular vibrations present in the material and it shows that the sharpest apex at 508 cm^{-1} obtained is attributed to the stretching oscillations of Fe–O and V–O–V modes. The Raman spectrum confirmed the separation of Fe − O, V − O, and different stretching fashions of V − O − Fe. The V–O stretching mode increases the intense bands showing the very high strongest peak of $FeVO_4$ because of electro negativity of iron the metal. The morphology of iron vanadate was confirmed with SEM analysis showing that particles are much isolated and cubical with few polyhedron structures. The electrochemical response of $FeVO_4$ evaluated the specific capacitance at 10 mV/s as 402 Fg^{-1}Energy density values were calculated as 16.08 $Whkg^{-1}$, 13.08 $Whkg^{-1}$, 10.2 $Whkg^{-1}$, 8.76 $Whkg^{-1}$, 7.64 $Whkg^{-1}$ and 6.92 $Whkg^{-1}$ from the cyclic voltammetry profile at the slow rates varying from 10 −100 mV/s. The magnetic properties were analyzed by measuring the magnetic susceptibility and magnetization using a VSM magnetometer and the results evident that the material exhibits the paramagnetic behavior.

1. Introduction

Recently, energy storage devices such as supercapacitors, fuel cells and Li-ion batteries have gained much attention among researchers owing to the exponential growth of global population as a consequence of major energy crisis. Due to their appealing characteristics like high power density, long cycle life, etc., supercapacitors are considered as one of the most recent developments in the field of energy storage and conversion devices (Nithya et al., 2011; Deng et al., (2008); Mangamma et al., 1996). On the other hand, the energy density of supercapacitors is still lower than batteries, which limits their practical applications (Vuk et al., 2002; He et al., (2008)). Hence, proper selection of electrode materials is

* Corresponding author.
E-mail addresses: mawad@ksu.edu.sa (M.A. Awad), AAHindi@pnu.edu.sa (A.A. Hendi), saronataraj@gmail.com (S. Natarajan), Ortashi9@ksu.edu.sa (K.M.O. Ortashi), saralsaif@ksu.edu.sa (S.S.A. Alsaif), 444204403@student.ksu.edu.sa (R.A. Alnamlah), rabeer@KSU.EDU.SA (A. Rasheed), haathbaita@KSU.EDU.SA (H. Althobaiti).

Peer review under responsibility of King Saud University.

Production and hosting by Elsevier

https://doi.org/10.1016/j.jksus.2023.102857
1018-3647/

important to counter balance the charges and to obtain the finer electrochemical performance. Until now, plenty of orthovandates ($BiVO_4$, $CeVO_4$, $ZnVO_4$, $MnVO_4$, and $CuVO_4$) were synthesized and employed as electrode materials for supercapacitor applications. Metal oxide nanoparticles were also utilized as electrodes to enhance the super capacitive performance. Sethuraman et al. have prepared Fe_2O_3/C nanocomposites based negative electrode which delivers a specific capacitance of 315F/g in 2 M KOH electrolyte in the potential range of 0.2 to −0.7 V at 2 mV s^{-1} (Sethuraman et al., 2014). Similarly, Ghulam Mustafa and co-workers have prepared Mn_2O_3/Graphene based composite materials exhibited a specific capacitance of 391F/g at a scan rate of 5 mV/s (Mustafa et al., 2021). Conversely, Mn_3O_4 was employed as a positive electrode which delivered the specific capacitance of 232.5 F g^{-1} at 0.5 A g^{-1} in the potential range of 0 to + 1.0 V and MnO_2 provided a specific capacitance of 411.9 F g^{-1} at 0.25 A g^{-1} in the potential range of −0.2 to + 0.8 V (Nithya et al., 2015). To the best of our knowledge, $FeVO_4$is a promising material to resolve all these electrochemical issues. Vanadium exists stable in oxidation states varying from + 2 to + 5, and combines with various elements to produce several new compounds. $FeVO_4$ occurs in four types of polymorphs: $FeVO_4$-I, $FeVO_4$-II, $FeVO_4$-III and $FeVO_4$-IV. Among these polymorphs, only $FeVO_4$ – I is stable at room temperature and remaining phases are not. They exist in metastable state at intense temperature and pressure. In $FeVO_4$-I, Fe^{3+} ions consists three crystallographic positions. Two of this positions are deformed octahedral FeO_6 and one site occurs in perverted triangular bipyramidal FeO_5 domains. The octahedral Fe-O forms six vertical lines of two fold hooked sequence. These sequences are combined mutually by VO_4 triangular pyramids which in turn generate three dimensional sub-structures (Groń et al., 1991; Mishra et al., 2019; Quan et al., 2016). Previously, Aradhya Mishra et al. have utilized $FeVO_4$ and $FeVO_4$/rGO composites provided a specific capacitance value of 97.54F/g and 189.10F/g at 0.5 mA/cm^2, respectively (Aladine et al., 2009). So far, $FeVO_4$ particles had been synthesized using several techniques such as, wet chemical route, flux method and hydrothermal method for magnetic, electrical and photocatalytic applications(Groń et al., 1991; Melghit and Mungi, 2007; Poizot et al., 2000; Sim et al., 2012; Kesavan et al., 2021). The objective of the present work is to synthesis $FeVO_4$ nanoparticles utilizing simple wet chemical co-precipitation route by modifying the pH of the suspension with the help of ammonia solution and to study its electrochemical and magnetic characteristics.

2. Experimental section

The FeVO4 nanoparticles were synthesized by traditional wet chemical methodusing ferric nitrate Fe(NO3)3 9H2O, ammonium meta vanadate (NH4VO3) as the starting precursor. For the synthesis of $FeVO_4$, 0.1 M of ferric nitrate and0.1 M of ammonium meta vanadate was dissolved in de-ionized water individually under constant stirring. Ammonium meta vanadate solution was prepared at a temperature of 70 °C as it has low solubility at room temperature. Ferric nitrate solution was mixed drop by drop into the ammonium meta vanadate mixtureand swirled vigorously for 2 h. The pH of the suspension was sustained with the value of 3 by adding 0.01 M ammonia solution. To remove the organic residuals present in the precipitate, it was cleaned by using de-

$$Fe(NO_3)_3.9H_2O + NH_4VO_3 + NH_4OH \rightarrow FeVO_4 + 2NH_4NO_3 + HNO_3 + 9H_2O$$

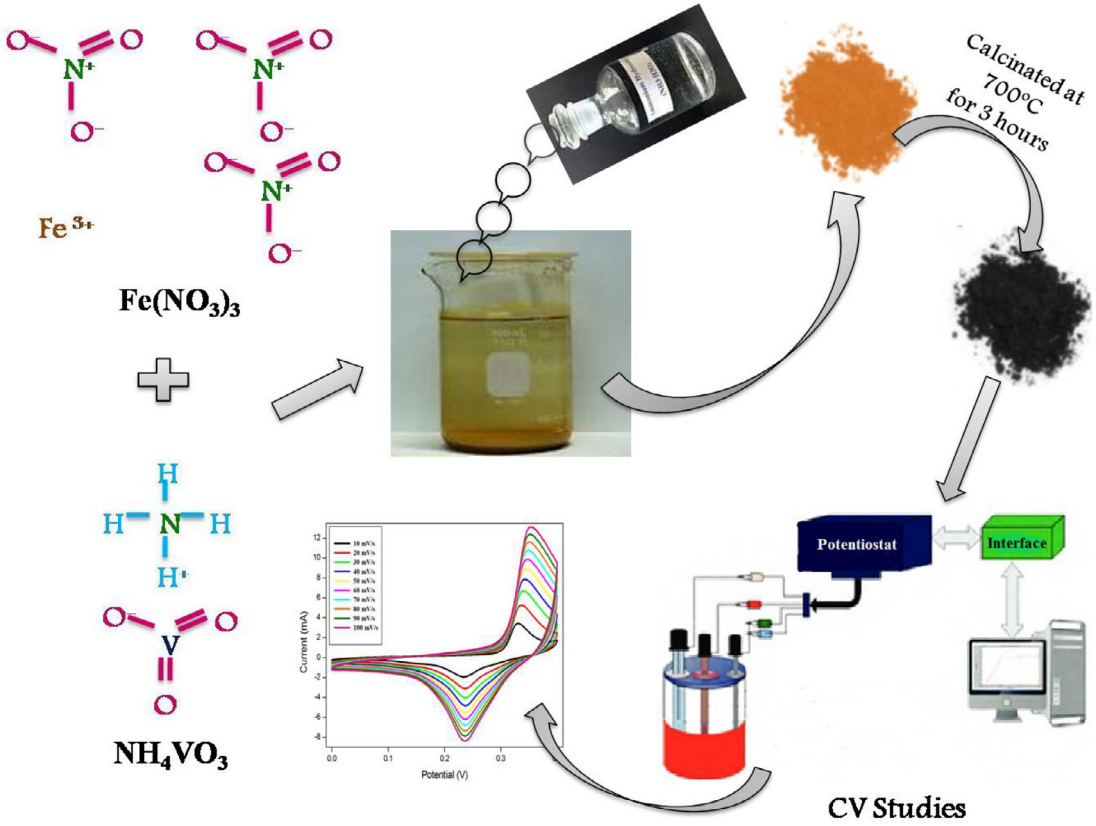

Fig. 1. Graphical representation for the synthesis schemeof $FeVO_4$ nanoparticles.

ionizedwater again and again. The end product was dehydratedin hot plate at 60 °C for 5 h and then grinedusing agate mortar. The pulverized sample was calcinated at 700 °C for 3 h. Fig. 1 shows the graphical illustration of the synthesis process of $FeVO_4$ nanoparticles. The reaction mechanism as follows:

$$\mathbf{Fe(NO_3)_3.9H_2O + NH_4VO_3 + NH_4OH \rightarrow FeVO_4 + 2NH_4NO_3 + HNO_3 + 9H_2O}$$

3. Characterizations

Powder X-ray diffraction (XRD) pattern was took down from an X'Pert PRO diffractometer having CuKα target (λ = 1 1.5406 Å5406 Å) at room temperature (RT). The intensity data were taken by uninterrupted scanning in θ–θ manner from 10° to 80°. Perkin Elmer spectrometer of KBr pellet technique was employed to record the Fourier-transform infrared (FTIR) spectrum in the zone of 4000 – 400 cm^{-1}at room temperature. Vibrations of the molecules were also complemented with Raman spectra using Horiba-Raman Spectrometer. Carl Zeiss EVO 18 instrument was utilized to identify the morphology of the nanoparticles. Princeton Applied Research Versa STAT MC cyclic voltameter / impedance analyzer was used to analyze the electrochemical response and EIS behaviour of $FeVO_4$ nanoparticles. The magnetic behavior of the as-prepared material is characterized using vibrating sample magnetometerat a magnetic field of −2 to + 2(cryogenic, UK).

3.1. Electrode preparation

The working electrode was fabricated by combining the materials including $FeVO_4$, carbon black, and PVDF (Polyvinylidene difluoride) in a weight ratio of 80:10:10 followed by an appropriate quantity of NMP (N-Methyl-2-pyrolidone) were added, and grinded to form homogenous slurry. The resultant slurry was coated on the nickel foam (1x2 cm^2) and dried in vacuum oven for 12 h at 80 °C.

4. Results and discussion

XRD pattern was acquired to determine crystal properties of the synthesized $FeVO_4$ NPs. Fig. 2 displays the XRD pattern of the $FeVO_4$ nanoparticle. From the spectrum, it is clear that the diffraction peaks located at 16.72(011), 17.72(−111), 20.27(110), 23.13 (0–21), 23.50(-1–12), 23.96(−112), 25.19(012), 27.27(−201), 27.65(−211), 27.93(1–12), 28.26(−210), 28.78(200), 29.49 (−103), 30.17(120), 30.49(−212), 31.01(-1–13), 31.43(-2–11), 32.33(2–11), 33.56(201), 34.93(−203), 35.41(−222), and 42.45°(0–33) crystal planes of triclinic $FeVO_4$ (JCPDS no. 71–1592) has noany impurities. The formation of pristine $FeVO_4$ was confirmed from the obtained results, which agrees with the ICDD Database (JCPDS no. 71–1592) and alsoverified the occurrence of the substance in a single pureform without any secondary phases. The obtained results are well in agreement with theprior reports (Sethuraman et al., 2014). The material attains its major growth in the (012), (−201), and (1–12) planes which will be confirmed from the strong intensity obtained in that corresponding direction. For the synthesized $FeVO_4$, the XRD shows a high peak intensities and high degree of crystallinity analogous to the obtained peaks. Strong crystal planes were formed at Miller indices(111), (0–12), and (−220) which is confirmed from the intensity of the diffraction peaks. The average crystalline size (Scherrer equation), microstrain and dislocation density of the formed $FeVO_4$nanocatalysts is calculated by using the formulae given below (Mostafa and Amdeha, 2022) and were tabulated in Table 1.

Crystallite size 'D'

$$D = \frac{0.89\lambda}{\beta cos\theta} \quad (1)$$

Microstrain 'ϵ'

$$\epsilon = \frac{\beta \cos\theta}{4} \quad (2)$$

Dislocation density 'δ'

Table 1
Crystallite size, Microstrain and Dislocation density of $FeVO_4$ nanoparticles.

Crystallite Size 'D' (nm)	35.11
Microstrain 'ε' X 10^4 (lin^{-2} m^{-4})	14.96
Dislocation Density 'δ' X 10^{14} (lines/$meter^2$)	12.69

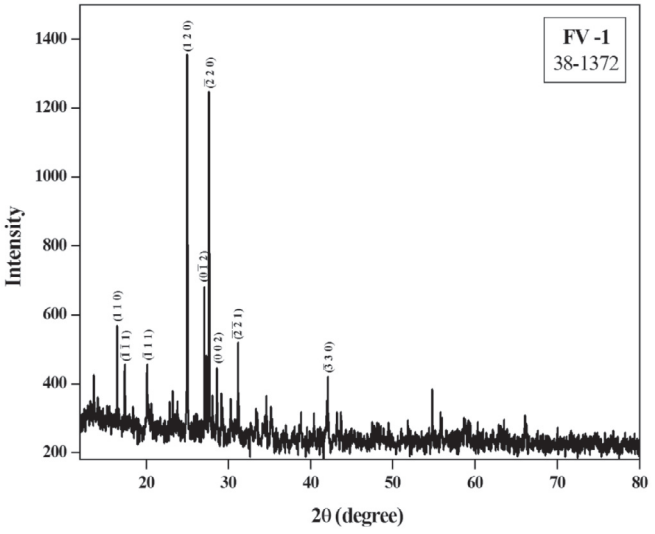

Fig. 2. XRD pattern of the synthesized $FeVO_4$ nanoparticles.

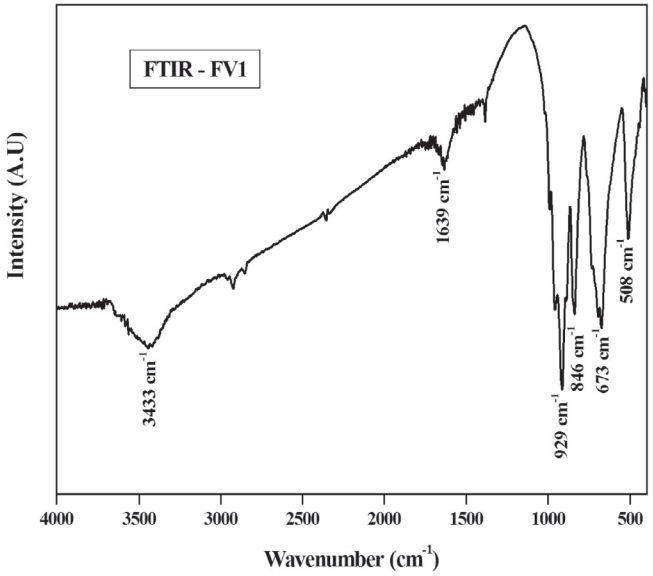

Fig. 3. FTIR analysis of the synthesized $FeVO_4$ nanoparticle.

$$\delta = \frac{1}{D^2} \quad (3)$$

where λ is the wavelength of the X-ray source; θ is the Bragg's angle and β is the value of the full width half maximum.

The $FeVO_4$ nanoparticle was subjected to FT-IR analysis to identify the molecular vibrations in the form ofnano-catalysts. Fig. 3 shows the peaks obtained for $FeVO_4$ nanoparticles were clear intensified bands, proposing the complete formation of appropriate chemical bonds (Nithya and Kalai Selvan, 2011). The apexat 3000–––3500 $cm^{-1}$is ascribedto the O–H stretching vibration of the ingested water. The bending vibration of H_2O molecules is confirmed from the absorption peak at 1639 cm^{-1}. In addition, two more bands were observed, one is sharpest at 846 and the other at 929 cm^{-1} was consigned to andasymmetric stretching oscillations of V–O respectively. Mixed bridging of V-O-Fe stretching was observed from sharp peak at 673 cm^{-1}. The sharpest apex at 508 cm^{-1} obtained is attributedto the stretchingoscillations of Fe–O and V–O–V modes, these result are similar to those reported by (Nguyen and Thanh, 2014; He et al., 2020).

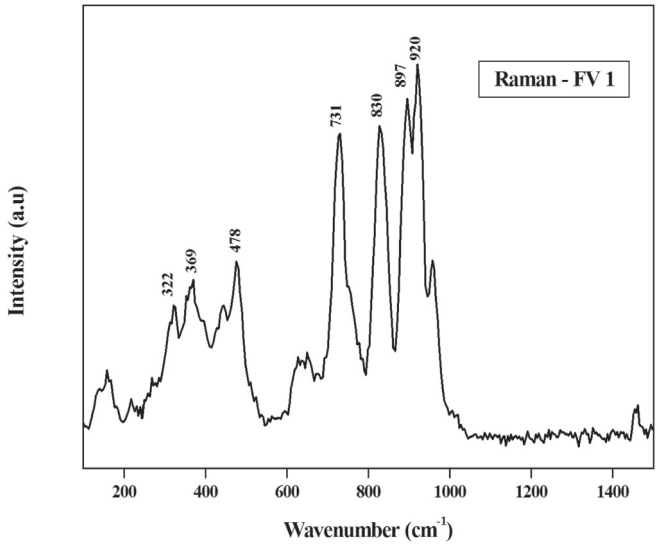

Fig. 4. Raman spectrum of the as-prepared $FeVO_4$ nanoparticles.

Raman spectroscopy was used to prove the occurrence of crystalline nature. Raman spectrum performed at the normal temperature (Fig. 4). The well-defined peaks were obtained at 322, 369, 478, 731, 830, 897, and 920 cm^{-1}. The spectrum more evidently shows the crystallization property. The Raman spectrum confirmed the separation of Fe – O, V – O, and different stretching fashions of V – O – Fe. Zhang and his co-authors suggested that the peak ataround 830 cm^{-1} was allocated to V– O stretching modes, and no splitting in the band represents the existence of degeneracy in the VO_4 tetrahedron symmetric stretching vibration.

The V–O stretching mode increases the intense bands showing the very high strongest peak of $FeVO_4$ because of electro negativity of iron the metal. The significant peaks obtained at lower frequencies from 200 to 400 cm^{-1} are because of the V – O – V contortions and Fe – O stretching. The spanning V – O···Fe stretching oscillationwas confirmed from the apexes at 731 and 830 cm^{-1}. The definitive apexes at 897 and 920 cm^{-1} are because of the stretching vibration of the terminal V – O stretching as reported by (Sethi et al., 2020; Yuan et al., 2012; Zhang et al., 2015). The spectrum of Raman bands of synthesized $FeVO_4$ shows many bands due to the triclinic structure of $FeVO_4$, and non degenerate vibrations (Zhou and Li, 2012). The lower wave number bands were occurred due to the external modes of the lattice, vibrational and translational motions (Wang et al., 2022). From a crystalline point of view, all nanoparticles were compiled of V–O polyhedrons and some other metal–oxygen polyhedrons (Morton et al., 2010; Atta and Abdelhamied, 2021).

Fig. 5 represents the SEM micrograph of $FeVO_4$ nanoparticles obtained by calcinating at 700 °C. From the SEM image, it is evident that the particles are muchisolatedand cubical with few polyhedronstructures. The SEM image contributes to the formation of regular polyhedron shape of $FeVO_4$ nanocatalysts (Zhu et al., 2014). At

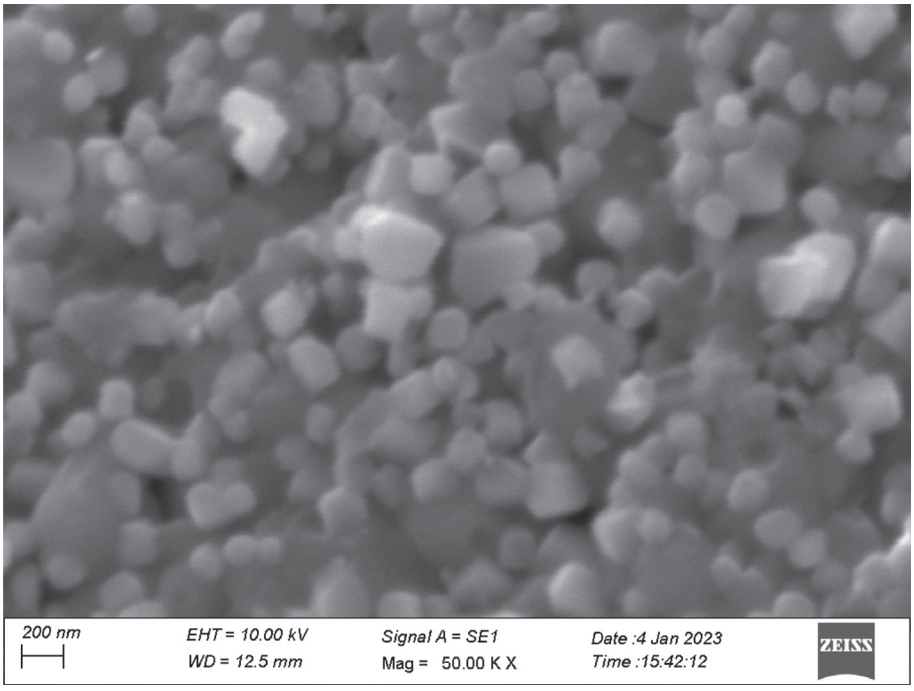

Fig. 5. SEM micrograph of as prepared $FeVO_4$ nanocatalysts.

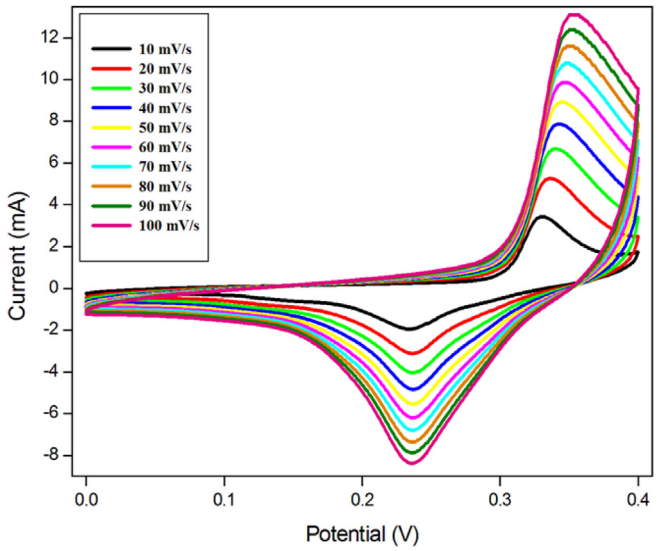

Fig. 6. CVcurves for $FeVO_4$ super capacitor under KOH electrolyte.

some regions, the bigger nanoparticles are bounded by smaller nanoparticles.

Fig. 6 shows the cyclic voltammetry of the $FeVO_4$ nanoparticles under 2 M of KOH electrolyte. The cyclic voltammetry studyis performed under slow rate varying from 10 to 100 mV/s. With increasing the scan rate, there is an increase in cyclic behaviour which is frequent in super capacitor behaviour. This is associated to the insufficient flow rate for the electrolyte ions to dispersein to the stomas of the nanoparticles (Ahmed Mohamed et al., 2020 Jul; Zhi Qiang He, 2020).

The cyclic curves have a good surface area which results in the great capacitance value and provide evidences of the electrochemical behavior of the supercapacitor (Nithya et al., 2015; Zhu et al., 2012). The specific capacitance is computed by the relation

$$C_p = \frac{\int I\,dV}{2km\Delta V}$$

Where $\int I\,dV$ is the integral area, k is the slew rate, m is the mass of the active substance and ΔV is the difference in the potential. The value of specific capacitance at 10, 20, 40, 60, 80 and 100 mV/s is 402 Fg^{-1}, 327 Fg^{-1}, 255 Fg^{-1}, 216 Fg^{-1}, 191 Fg^{-1} and 173 Fg^{-1} respectively. At lower scan rates, the specific capacitance is very high, whereas at higher scan rates it goes on decreasing.

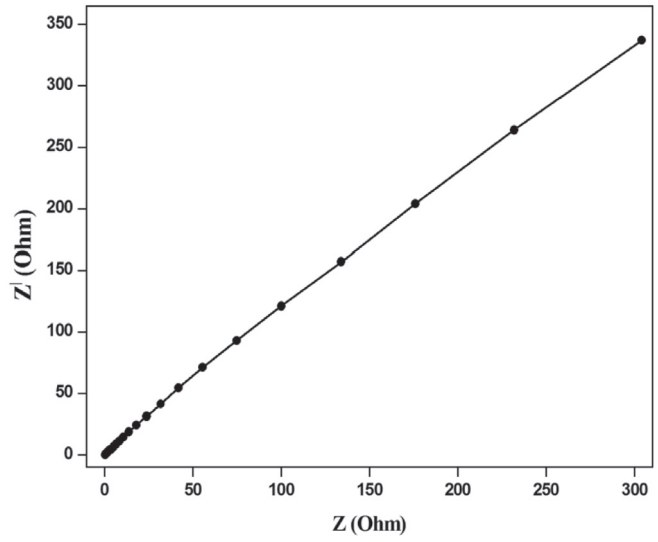

Fig. 7. Electrochemical Impedance Spectral curve for $FeVO_4$.

Fig. 7 shows the electrochemical impedance nature of $FeVO_4$is recordedutilizing electrochemical impedance spectroscopy (EIS) in the frequency spanfrom 10 mHz to 1 MHz. Avery small and weakarc with a major single upright line was obtained at high frequency. The arcfeatures to the charge transfer resistance (R_{CT}). Subsequently, the equivalent series resistance (R_S) is the meeting point of the impedance lineon the real locusin the region of intense frequency. The series resistance is the mixture of three different resistances: natural resistance of the active substance, junction resistance at the active substance / current collector interface and ionic resistance of the electrolyte (Han et al., 2013; Li et al., 2014; Wang et al., 2016).

The energy density (E) is calculated from the following relation and its value depends on C_S, potential values V_{max} and V_{min}.

$$E = \frac{C_s\left(V_{max}^2 - V_{min}^2\right)}{2}$$

The energy density values are found to be 16.08 $Whkg^{-1}$ at the slow rate of 10 mV/s, 13.08 $Whkg^{-1}$ at 20 mV/s, 10.2 $Whkg^{-1}$ at 40 mV/s, 8.76 $Whkg^{-1}$ at 60 mV/s, 7.64 $Whkg^{-1}$at 80 mV/s and 6.92 $Whkg^{-1}$ at 100 mV/s.

Fig. 8 clearly shows the specific capacitance of $FeVO_4$ nanoparticlesis found to be 374.6, 237.5 and 134.9 Fg-1 at 1, 3and 5 Ag-1 respectively. It is found that the specific capacitance is decreased with increasing the current density. The Comparison of electrochemical performance of prepared material with other reported materials as shown in Table 2.

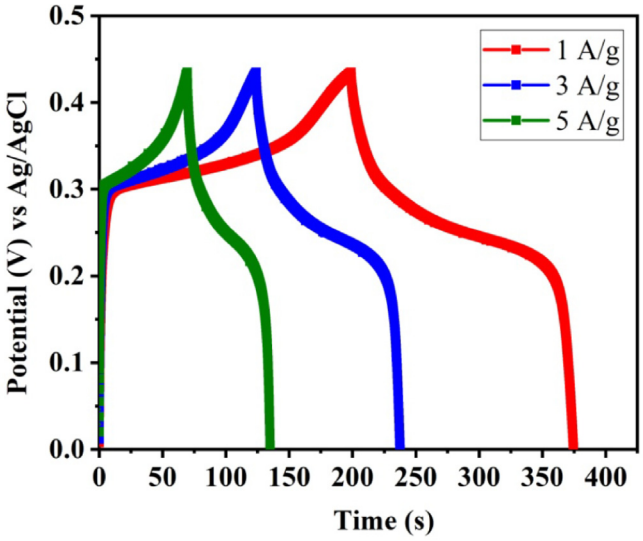

Fig. 8. Charge-discharge curve of $FeVO_4$ nanoparticles for different A/g values.

Table 2
Comparison of electrochemical performance of prepared material with other reported materials.

Material	Electrolyte	Specific capacitance (F/g)	Ref.
Mn3O4	1 M of KOH	355	31
Ni-Mn3O4	1 M Na2SO4	230	32
Graphene/Mn3O4	1 M Na2SO4	147	33
NiFe2O4	2 M KOH	368	34
FeVO4	2 M KOH	374.6	Present work

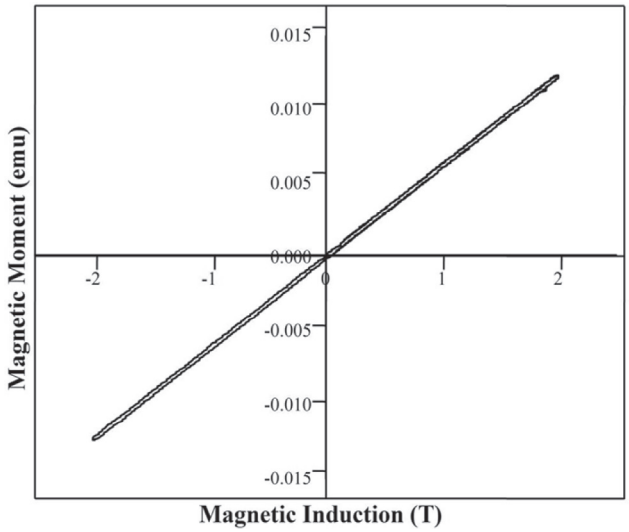

Fig. 9. Magnetic curve for $FeVO_4$ shows the plot of magnetic induction (T) vs magnetic moment (μ) for the iron vanadate.

The investigation into the magnetic properties of FeVO4 was carried out with the purpose of gaining a better comprehension of the influence that the surfactant has on the magnetic properties of the material. The VSM magnetic measurements for the as prepared FeVO4 NPs in Fig. 9 show the magnetic properties of resulting nanoparticles. Magnetization is the degree to which an applied magnetic field aligns magnetic dipoles inside a material. Samples exhibit a linear relationship, and the magnetic moments are not saturated up to an applied field of 50 kOe. It's possible that the samples' well defined magnetic ordering is responsible for the observed linear behavior. This might be because of the surfactant's role in producing a magnetic structure that is properly aligned. In the case of transition metal oxides paramagnetic behavior exists at high temperatures and exhibits ordered magnetic structures at low temperatures. Antiferromagnetic materials have the spins in the antiparallel direction so that the net magnetic moment is zero (Nithya et al., 2011). The FeVO4 nanoparticles exhibit paramagnetic behaviour at room temperature, with a saturation magnetization of 0.0015 $emug^{-1}$. From the graph, it is evident that the material exhibits the paramagnetic behaviour.

5. Conclusion

Metal oxide nanoparticles were also utilized as electrodes to enhance the super capacitive performance. This study examined the potential work of $FeVO_4$ nano-catalysts were successfully synthesized employing wet chemical process with a controlled pH value using ammonia solution. Thus, it has advantage of producing high-purity materials with favorable stoichiometry, a very homogenous product, and enhanced reactivity at lower temperatures, all without the need for complex equipment. The material attains its major growth in the (012), (−201), and (1–12) planes which will be confirmed from the strong intensity obtained in that corresponding direction. The significant peaks obtained at lower frequencies from 200 to 400 cm^{-1} are because of the V − O − V contortions and Fe − O stretching. The lower wave number bands were occurred due to the external modes of the lattice, vibrational and translational motions. The spectrum of Raman bands of synthesized $FeVO_4$ shows many bands due to the triclinic structure of $FeVO_4$, and non– degenerate vibrations. The SEM image contributes to the formation of regular polyhedron shape of $FeVO_4$-nano-catalysts. At some regions, the bigger nanoparticles are bounded by smaller nanoparticles. In order to acquire cyclic voltammetry study, the $FeVO_4$ nanocatalyst was coated in nickel foam by doctor blade technique. The specific capacitance and energy density values are found to be 402 Fg^{-1} and 16.08 $Whkg^{-1}$ at a scan rate of 10 mV/s, 327 $Fg^{-1}$and 13.08 $Whkg^{-1}$ at 20 mV/s, 255 Fg^{-1} and 10.2 $Whkg^{-1}$ at 40 mV/s, 216 Fg^{-1} and 8.76 $Whkg^{-1}$ at 60 mV/s, 191 Fg^{-1} and 7.64 $Whkg^{-1}$ at 80 mV/s, 173 Fg^{-1} and 6.92 $Whkg^{-1}$ at 100 mV/s from cyclic voltammetry and electrochemical impedance spectral analysis. From the results obtained, one can say the controlled pH with ammonia solution has sufficiently increased the super capacitance value of $FeVO_4$ when compared with other reported literatures.

Declaration of Competing Interest

The authors declare that they have no known competing financial interests or personal relationships that could have appeared to influence the work reported in this paper.

Acknowledgments

The authors extend their appreciation to the Deputyship for Research and Innovation, "Ministry of Education" in Saudi Arabia for funding this research (IFKSUOR3–078-1).

References

Ahmed Mohamed, H.E., Afridi, S., Khalil, A.T., Zohra, T., Ali, M., Alam, M.M., Ikram, A., Shinwari, Z.K., Maaza, M., 2020. Phyto-fabricated Cr_2O_3 nanoparticle for multifunctional biomedical applications. Nanomedicine (Lond.) 15 (17), 1653–1669. https://doi.org/10.2217/nnm-2020-0129.

Aladine, D.A., Kundys, B., Martin, C., Radaelli, P.G., Brown, P.J., Simon, C., Chapon, L. C., 2009. Multiferroicity and spiral magnetism in FeVO4 with quenched Fe orbital moments. Phys. Rev. B 80, 4. https://doi.org/10.1103/PhysRevB.80.220402. 220402(R).

Atta, A., Abdelhamied, M.M., Essam, Doaa, Shaban, Mohamed, Alshammari, Alhulw H., Rabia, Mohamed, 2021. Structural and physical properties of polyaniline / silver oxide / silver nanocomposite electrode for supercapacitorapplications. Intl J Energy Res. 133,. https://doi.org/10.1002/er.7608 108926.

Deng, J., Jiang, J., Zhang, Y., Lin, X., Du, C., Xiong, Y., 2008. FeVO4 as a highly active heterogeneous Fenton-like catalyst towards the degradation of Orange II. Appl. Catal. B 84, 468–473. https://doi.org/10.1016/j.apcatb.2008.04.029.

Groń, T., Krok-Kowalski, J., Kurzawa, M., Walczak, J., 1991. Electrical conductivity in the antiferromagnetic compounds $FeVO_4$, $FeVMoO_7$ and $Fe_4V_2Mo_3O_2$. J. Magn. Magn. Mater. 101 (1–3), 148–150. https://doi.org/10.1016/0304-8853(91)90708-I.

Han, D., Pengcheng, X.u., Jing, X., Wang, J., Song, D., Liu, J., Zhang, M., 2013. Facile approach to prepare hollow core–shell NiOmicrospherers for supercapacitor electrodes. J. Solid State Chem. 203, 60–67. https://doi.org/10.1016/j.jssc.2013.04.009.

He, Z., Yamaura, J.I., Ueda, Y., 2008. Flux Growth and Magnetic Properties of FeVO4 Single Crystals. J. Solid State Chem. 181, 2346–2349. https://doi.org/10.1016/j.jssc.2008.05.041.

He, X., Zhang, C., Tian, D., 2020. The Structure, Vibrational Spectra, and Thermal Expansion Study of AVO_4 (A=Bi, Fe, Cr) and $Co_2V_2O_7$. Materials (Basel). 13 (7), 1628. https://doi.org/10.3390/ma13071628.

Kesavan, G., Pichumani, M., Chen, S.M., 2021. Influence of crystalline, structural, and electrochemical properties of iron vanadate nanostructures on flutamide detection. ACS Applied Nano Materials 4 (6), 5883–5894. https://doi.org/10.1021/acsanm.1c00802.

Li, O., Wei, J., Qian, Y., Zhang, J., Jian, Y.u., Wang, G., Guangwen, X.u., 2014. Effects of the graphene content and the treatment temperature on the supercapacitive properties of VOx/graphene nanocomposites. Colloids Surf A Physicochem Eng Asp 449, 148–156. https://doi.org/10.1016/j.colsurfa.2014.03.001.

Mangamma, G., Prabhu, E., Gnanasekaran, T., 1996. Investigations on $FeVO_4$ as a gas sensor material. Bull. Electrochem. 12 (11-12), 696–699.

Melghit, K., Mungi, A.S., 2007. New form of iron orthovanadate $FeVO_4{\cdot}1.5H_2O$ prepared at normal pressure and low temperature. Mater. Sci. Eng. B 136 (2), 177–181. https://doi.org/10.1016/j.mseb.2006.09.028.

Mishra, Aradhya, Bera, Ganesh, Priyanath Mal, G., Padmaja, Pintu Sen, Das, Pradip, Chakraborty, Brahmananda, Turpu, G.R., 2019. Comparative electrochemical analysis of rGO-FeVO4 nanocomposite and FeVO4 for supercapacitor application. Appl. Surf. Sci. 488, 221–227. https://doi.org/10.1016/j.apsusc.2019.05.259.

Morton, Craig D., Slipper, Ian J., Thomas, Michael J.K., Alexander, Bruce D., 2010. Synthesis and characterisation of Fe–V–O thin film photoanodes. J. Photochem.

Photobiol. A Chem. 216 (2–3), 209–214. https://doi.org/10.1016/j.jphotochem.2010.08.010.
Mostafa, E.M., Amdeha, E., 2022. Enhanced photocatalytic degradation of malachite green dye by highly stable visible – light – responsive Fe-based tri-composite photocatalysts. Environ SciPollut Res 29, 69861–69874. https://doi.org/10.1007/s11356-022-20745-6.
Mustafa, G., Mehboob, G., Khisro, S.N., Javed, M., Chen, X., Ahmed, M.S., Ashfaq, J.M., Asghar, G., Hussain, S., Rashid, A.U., Mehboob, G., 2021. Facile Synthesis and Electrochemical Studies of Mn_2O_3/Graphene Composite as an Electrode Material for Supercapacitor Application. Front Chem. 9. https://doi.org/10.3389/fchem.2021.717074.
Nithya, V.D., Kalai Selvan, R., 2011. Synthesis, electrical and dielectric properties of $FeVO_4$ nanoparticles. Physica B: Condensed Matter 406 (1), 24–29. https://doi.org/10.1016/j.physb.2010.10.004.
Nithya, V.D., Kalai Selvan, R., Sanjeeviraja, C., Mohan Radheep, D., Arumugam, S., 2011. Synthesis and characterization of $FeVO_4$ nanoparticles. Mater. Res. Bull. 46, 1654–1658. https://doi.org/10.1016/j.materresbull.2011.06.005.
Nithya, V.D., Pandi, K., Lee, Y.S., Kalai Selvan, R., 2015. Synthesis, characterization and electrochemical performances of nanocrystalline $FeVO_4$ as negative and $LiCoPO_4$ as positive electrode for asymmetric supercapacitor. ElectrochimicaActa 167, 97–104. https://doi.org/10.1016/j.electacta.2015.03.107.
Poizot, P., Baudrin, E., Laruelle, S., Dupont, L., Touboul, M., Tarascon, J.M., 2000. Low temperature synthesis and electrochemical performance of crystallized $FeVO_4.1.1H_2O$. Solid State Ion. 138, 31–40. https://doi.org/10.1016/S0167-2738(00)00784-0.
Quan, Hongying, Cheng, Baochang, Xiao, Yanhe, Lei, Shuijin, 2016. One-pot synthesis of α-Fe2O3 nanoplates-reduced graphene oxide composites for supercapacitor application. Chem. Eng. J. 286, 165–173. https://doi.org/10.1016/j.cej.2015.10.068.
Sethi, M., Shenoy, U.S., Muthu, S., et al., 2020. Facile solvothermal synthesis of $NiFe_2O_4$ nanoparticles for high-performance supercapacitor applications. Front. Mater. Sci. 14, 120–132. https://doi.org/10.1007/s11706-020-0499-3.
Sethuraman, B., Purushothaman, K.K., Muralidharan, G., 2014. 1; Synthesis of mesh-like Fe2O3/C nanocomposite via greener route for high performance supercapacitors. RSC Adv. 4, 4631–4637. https://doi.org/10.1039/C3RA45025B.
Sim, D.H., Rui, X., Chen, J., Tan, H., Lim, T.M., Yazami, R., Hng, H.H., Yan, Q., 2012. Direct growth of $FeVO_4$nanosheet arrays on stsainless steel foil as high performance binder free Li-ion battery anode. RSC Adv. 2, 3630–3633. https://doi.org/10.1039/C2RA20058A.
Thanh, Nguyen T.K., Maclean, N., Mahiddine, S., 2014. Mechanisms of Nucleation and Growth of Nanoparticles in Solution. Chem. Rev. 114 (15), 7610–7630. https://doi.org/10.1021/cr400544s.
Vuk, A.S., Orel, B., Drazic, G., et al., 2002. UV-visible and IR spectrelectrochemical studies of $FeVO_4$ Sol-Gel Films for electrochromic Applications. J. Sol-Gel Sci. Technol. 23, 165–181. https://doi.org/10.1023/A:1013755618889.
Wang, Z., Jiang, Y., Yang, W., Li, A., Hunger, M., Baiker, A., Huang, J., 2022. Tailoring single site VO_4 on flame-made V/Al_2O_3 catalysts for selective oxidation of n-butane. J. Catal. 413, 93–105. https://doi.org/10.1016/j.jcat.2022.06.013.
Wang, Y., Song, Y., Xia, Y., 2016. Chem. Soc. Rev. 45, 5925. https://doi.org/10.1039/C5CS00580A.
Yuan, H.L., Yuan, B.H., Li, F., Liang, E.J., 2012. Phase transition and thermal expansion properties of $ZrV_{2-x}P_xO_7$. Acta Phys. Sin. 22,. https://doi.org/10.7498/aps.61.226502 226502.
Zhang, A.M., Liu, K., Ji, J.T., He, C.Z., Tian, Y., Jineng, F., Zhang, Q.M., 2015. Raman phonons in multiferroic $FeVO_4$ crystals. Chin. Phys. B 24,. https://doi.org/10.1088/1674-1056/24/12/126301 126301.
Zhi Qiang He, 2020. Dan Dan Chen, Min Wang, Chao Xiong Li, Xiang Ying Chen, Zhong Jie Zhang, Sulfur modification of carbon materials as well as the redox additive of Na_2S for largely improving capacitive performance of supercapacitors. J. Electroanal. Chem. 856,. https://doi.org/10.1016/j.jelechem.2019.113678 113678.
Zhou, K., Li, Y., 2012. Catalysis based on nanocrystals with well-defined facets. Angewandte Chemie International Edition 51 (3), 602–613. https://doi.org/10.1002/anie.201102619.
Zhu, X., Dai, H., Jing, H.u., Ding, L., Jiang, L.i., 2012. Reduced graphene oxide–nickel oxide composite as high performance electrode materials for supercapacitors. J. Power Sources 203, 243–249. https://doi.org/10.1016/j.jpowsour.2011.11.055.
Zhu, T., Zhou, J., Li, Z., Li, S., Si, W., Zhuo, S., 2014. Hierarchical porous and N-doped carbon nanotubes derived from polyaniline for electrode materials in supercapacitors. J Mater Chem A. 2 (31), 12545–12551. https://doi.org/10.1039/C4TA01465K.